

Research Article

Effect of Chloride Ions on Electrochemical Behavior of Canister Materials

Gha-Young Kim , Junhyuk Jang , Minsoo Lee , and Jin-Seop Kim 

Disposal Performance Demonstration Research Division, Korea Atomic Energy Research Institute, 111, Daedeok-Daero 989 Beon-Gil, Yuseong-Gu, Daejeon 34057, Republic of Korea

Correspondence should be addressed to Gha-Young Kim; gkim@kaeri.re.kr

Received 2 May 2022; Accepted 8 July 2022; Published 3 August 2022

Academic Editor: Jariah Mohamad Juoi

Copyright © 2022 Gha-Young Kim et al. This is an open access article distributed under the Creative Commons Attribution License, which permits unrestricted use, distribution, and reproduction in any medium, provided the original work is properly cited.

Various canister candidate materials (SS316L, Ti-Gr.2, Alloy 22, and Cu) were studied using groundwater at the Korea Atomic Energy Research Institute (KAERI) underground research tunnel (KURT), with the addition of chloride ions using different electrochemical techniques. The corrosion potential and corrosion current of test materials were obtained by the polarization measurement. The polarization measurements revealed that the addition of chloride ions was detrimental to the SS316L and Cu materials by increasing corrosion current, which is an indicator of corrosion rate. Impedance measurements and fitting analysis showed that the corrosion resistance of Cu was more than 10 times lower than that of other materials in the KURT groundwater solution containing 0.1 M of chloride ions.

1. Introduction

A metal canister, which enables the isolation of high-level radioactive waste and prevents its leakage, is regarded as the first barrier in a multi-barrier deep geological disposal system. Several countries have adopted different candidate materials for canisters according to the nature of the radioactive waste and the geological environment. Typically, a Cu canister with a cast-iron insert is used in Sweden and Finland; a Cu-coated steel vessel was designed in Canada, and an inner stainless-steel (SS316) cylinder with an outer alloy 22 cylinder and titanium drip shield is considered in the US as canisters [1–9]. The lifetime of a canister must be longer than at least 10^4 years, and it is significantly affected by geochemical environmental factors such as dissolved oxygen, chemical composition of groundwater, and temperature. In particular, the initial corrosion of canisters is caused by aggressive species in groundwater such as chlorides, sulfates, and nitrates [4]. Previously, we have reported the corrosion behavior of different canister materials (SS316L, Ti-Gr.2, Alloy 22, and Cu) in a Korean domestic repository environment [10].

In this study, we investigated the effect of chloride ions on the electrochemical behavior of the materials to extend the scope of our previous research [10] by comparing the corrosion potential and corrosion current of test materials and by calculating the polarization resistance through impedance fitting analysis. Chloride is known to be the most aggressive anion and strongly influences the corrosion behavior of metals. Therefore, NaCl was added to groundwater at the Korea Atomic Energy Research Institute (KAERI) underground research tunnel (KURT), and potentiodynamic measurements were performed to examine the corrosion potentials and currents of the test materials. Furthermore, electrochemical impedance spectroscopy was performed to observe the corrosion resistance ability of the canister materials.

2. Materials and Methods

Stainless steel 316L, titanium grade 2 (Ti-Gr.2), nickel alloy 22 (Alloy 22), and copper (Cu) were used as working electrodes (surface area: 1 cm^2). The chemical composition of the test materials used in this study is presented in Table 1.

TABLE 1: Chemical compositions of test materials used in this study.

Component (mg/kg)	Materials			
	SS316L	Ti-Gr.2	Alloy 22	Cu
Cu	2440	—	—	Remainder
Fe	Remainder	187	30000	—
Ti	—	Remainder	—	—
Si	426	894	800	160
Co	2014	1399	25000	166
W	—	579	30000	291
Zn	21	953	—	—
Sn	42	4	—	—
Sb	10	1	—	—
Pb	1	1	—	—
Mn	9752	—	5000	—
Nb	55	30	—	—
Mo	895	175	130000	—
Cr	174906	—	220000	—
Ni	79348	—	Remainder	—
V	885	46	3500	—
Zr	—	25	—	—
Ta	3	605	—	—

Before the experiment, the electrodes were polished with SiC paper (~2000 grit) and 0.15 μm alumina paste. Subsequently, the electrodes were sonicated in distilled water and dried. A saturated calomel reference electrode (SCE) and a Pt-mesh counter electrode were used to complete the cell. The electrolyte solution was KURT groundwater mixed with NaCl (0.1 M). The chemical composition of KURT groundwater has been reported previously [10]. A BioLogic SP-300 potentiostat/galvanostat with a typical three-electrode cell configuration was employed in the electrochemical experiment. All experiments were conducted at room temperature (25°C). Potentiodynamic polarization curves were obtained at a scan rate of 1 mV/s. Electrochemical impedance spectroscopy (EIS) measurements were performed at open circuit potential (OCP) by applying an AC signal of ± 10 mV amplitude RMS in the frequency range of 100 kHz to 10 mHz.

3. Results and Discussion

Figure 1 shows the polarization curves of the aforementioned four materials immersed in the chloride ion-added groundwater solution. Compared with the previous result obtained for KURT groundwater solution without the addition of 0.1 M NaCl [10], it is evident that the addition of chloride ions to the groundwater solution shifts the corrosion potential to more negative values for all materials. This increases the current density for materials, except Alloy 22. The polarization curve for SS316L shows obvious anodic behavior with a corrosion potential (E_{CORR}) of -0.230 V vs. SCE and a corrosion current (i_{CORR}) of $0.243 \mu\text{A}/\text{cm}^2$. As the electrode potential was increased above the corrosion potential, the anodic current increased gradually, followed by a rapidly increasing current near 0.6 V vs. SCE (pitting potential, E_{pit}). Ti-Gr.2 exhibited the highest E_{CORR} among the test materials and passivation characteristics, unlike other metals. The high corrosion resistance of titanium in an

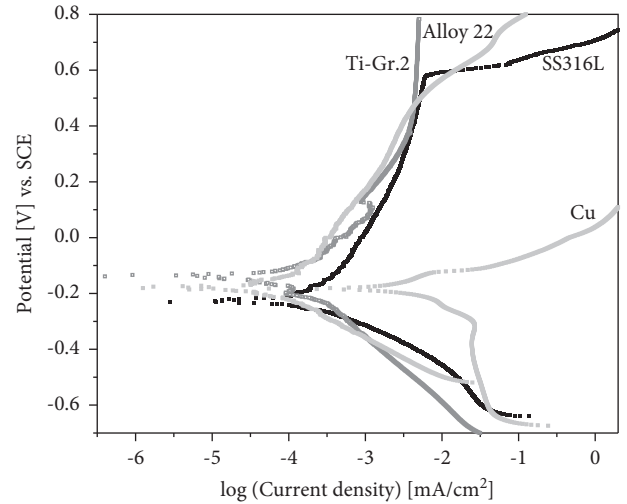


FIGURE 1: Potentiodynamic scans of SS316L, Ti-Gr.2, Alloy 22, and Cu in naturally aerated KURT groundwater with 0.1 M NaCl added.

aggressive environment is ensured by chemically stable oxide films such as TiO_2 [11]. Alloy 22 exhibited an E_{CORR} close to that of Cu, and the current density increased gradually as the potential increased. Cu showed a more apparent increase in corrosion current density than the other materials in the presence of chloride ions in the solution. It was also observed that the potential range decreased above the corrosion potential, wherein the anodic current density increased rapidly. This result shows the aggressiveness of chloride ions; the corrosion potential decreases, and the current density increases with the addition of chloride ions [12]. The corrosion potentials and currents of the test materials are listed in Table 2.

EIS measurements at the OCP were performed on the test materials (SS316L, Ti-Gr.2, Alloy 22, and Cu) by exposing them to the KURT groundwater solution, to which chloride ions were added. In the chloride-added KURT groundwater solution, a single capacitive semi-circle with a tail showing that the corrosion process was mainly charge transfer controlled [13] was found at SS316L, Ti-gr.2, and Alloy 22, whereas Cu exhibited more than one semi-circle (Figure 2). The comparison of arc radius in Figure 2 allows for a relative order of magnitude of corrosion resistance of materials [14]. In the presence of chloride ions, it was confirmed that the corrosion resistance of Ti-Gr.2 was relatively low compared to SS316L, which coincided with the previous study [15]. The three kinds of relaxation of Cu are clearly identified in Figure 3(a), which is quite similar to previous study [16]. The three time constants are attributed to the double-layer capacitance with charge transfer resistance, oxide layer-related capacitance in parallel with resistance, and reversible reactions or diffusion. The total impedance magnitude at intermediate frequency region can be attributed to the electrochemical corrosion reaction on metal surface. The total impedance magnitude of materials, immersed in the chloride-added KURT groundwater, in the low frequency range attributed to the electrochemical corrosion process was $\text{Cu} < \text{SS316L} < \text{Ti-Gr.2} < \text{Alloy 22}$ (Figure 3(b)).

TABLE 2: Corrosion potential and current of various canister materials in KURT groundwater solution with and without the addition of 0.1 M NaCl at 25°C.

	w/o 0.1 M NaCl [10]		w/ 0.1 M NaCl	
	E_{CORR} (V vs. SCE)	i_{CORR} ($\mu A/cm^2$)	E_{CORR} (V vs. SCE)	i_{CORR} ($\mu A/cm^2$)
SS316L	-0.198	0.124	-0.230	0.243
Ti-Gr.2	—	—	-0.136	0.124
Alloy 22	-0.175	0.224	-0.179	0.064
Cu	-0.048	0.938	-0.182	1.946

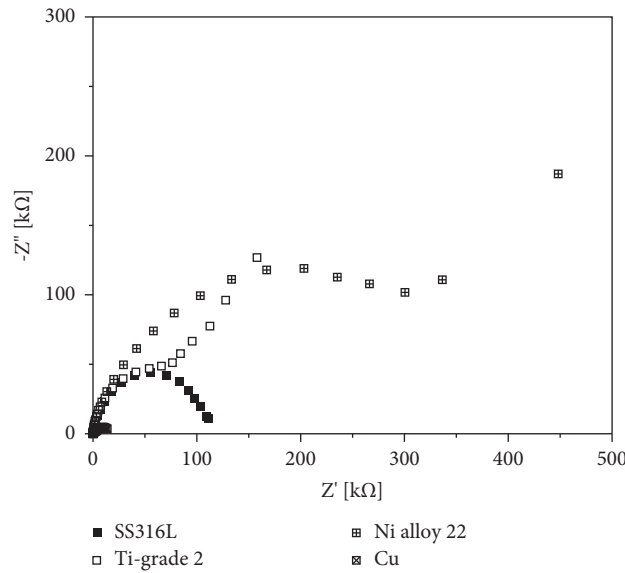


FIGURE 2: Nyquist plots of SS316L, Ti-Gr.2, Alloy 22, and Cu in naturally aerated KURT groundwater with the addition of 0.1 M NaCl.

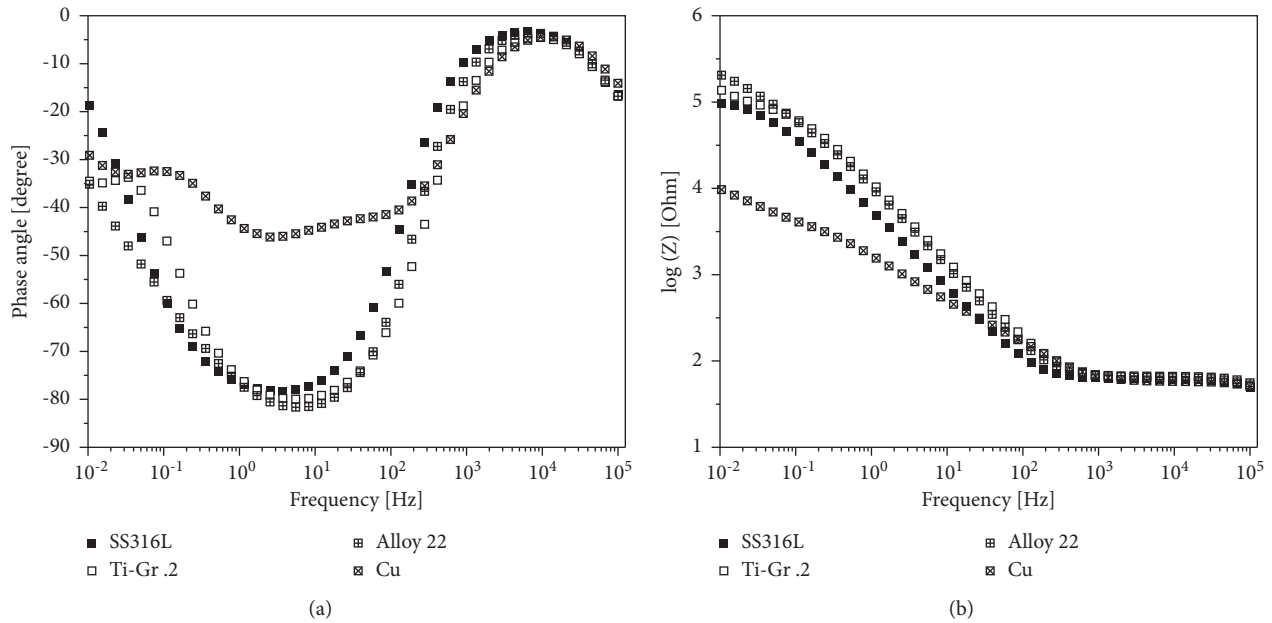


FIGURE 3: Bode plots of SS316L, Ti-Gr.2, Alloy 22, and Cu in naturally aerated KURT groundwater with the addition of 0.1 M NaCl.

The measured impedance data in the chloride-added groundwater solution were fitted using equivalent circuits (Figure 4) to quantify and compare the impedance

components of the test materials. The equivalent circuits were mostly used to elucidate the obtained data [16, 17]. In equivalent circuits, R represents the resistance, and Q

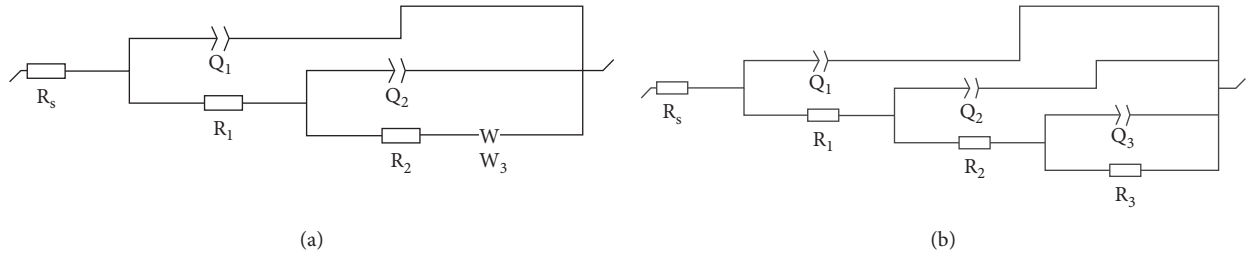


FIGURE 4: Equivalent circuits used to fit EIS spectra in chloride-added KURT groundwater solution for (a) SS316L, Ti-Gr.2, and alloy 22, and (b) Cu.

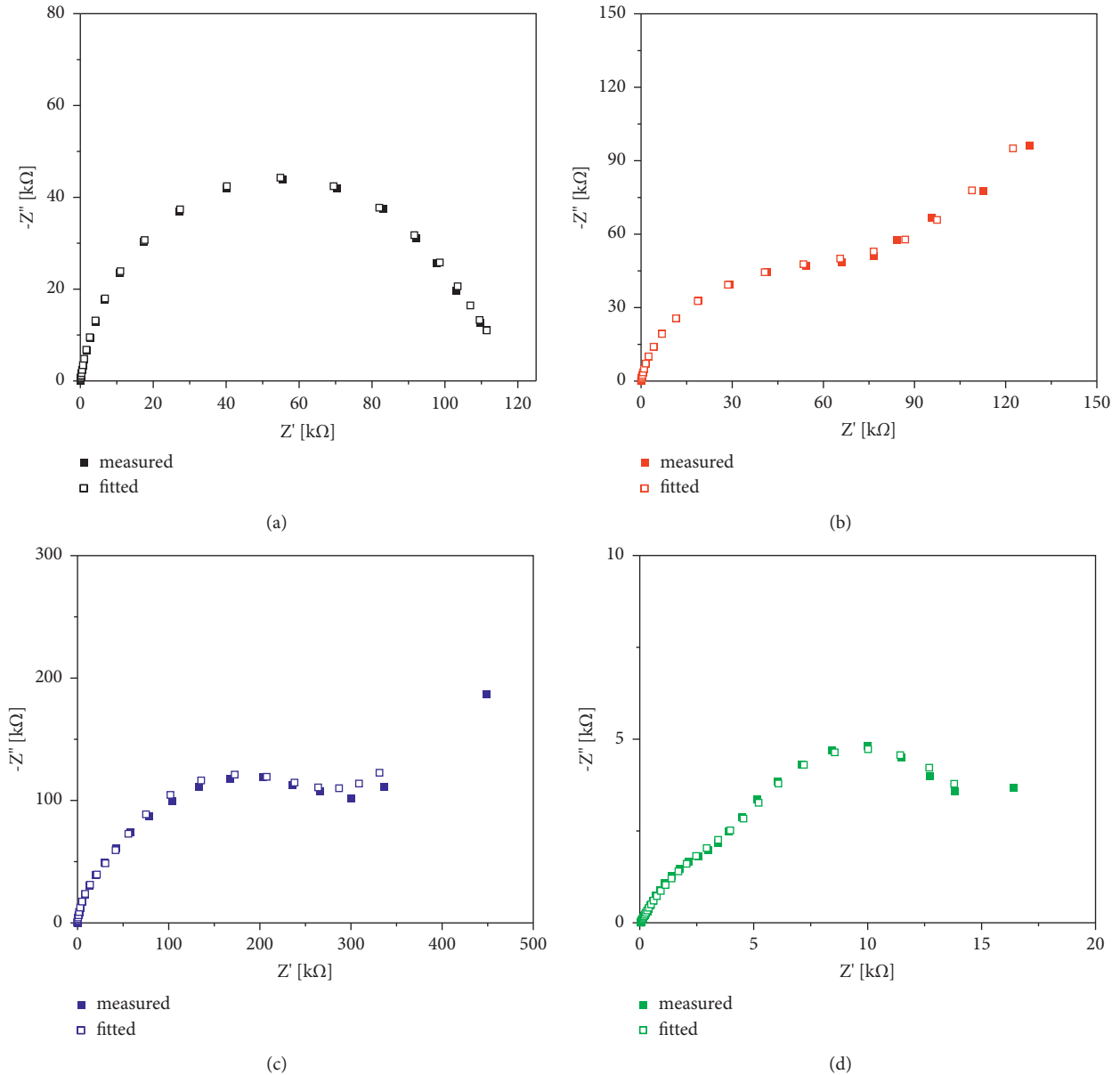


FIGURE 5: Measured and fitted data of impedance of (a) SS316L, (b) Ti-Gr.2, (c) Alloy 22, and (d) Cu in chloride-added KURT groundwater solution at 25°C.

represents the constant phase element (CPE), which was adopted to represent non-ideal capacitive behavior due to uneven current distribution or surface inhomogeneity. The CPE can be expressed as $Z_{CPE} = [Q(j\omega)^n]^{-1}$ ($j^2 = -1$),

where Q , ω , and n represent the CPE amplitude, angular frequency, and CPE exponent, respectively [18]. The value of n can be $0 \leq n \leq 1$, where 0 and 1 represent an ideal resistor and capacitor, respectively. The fitted curves are shown in

TABLE 3: R_p values of SS316L, Ti-Gr.2, Alloy 22, and Cu exposed to chloride-added KURT groundwater solution.

	SS316L	Ti-Gr.2	Alloy 22	Cu
R_p ($k\Omega\cdot\text{cm}^2$)	1.14×10^2	1.04×10^2	2.63×10^2	1.04×10^4

Figure 5. As mentioned above, three time constants were found in Cu (Figures 4(b) and 5(d)).

At the surface of the metal that is in contact with the chloride-containing solution, RC is related to the double-layer capacitance with charge transfer resistance [16, 17, 19–21], oxide film capacitance with resistance experienced by the ions while traveling through the oxide [22–24], and reversible reaction or diffusion process [25, 26]. Diffusion is replaced by Warburg impedance instead of an RC combination to describe mass transfer from or to the surface [17, 22]. For SS316L, Ti-Gr.2, and Alloy 22, the third component was fitted satisfactorily using a model with a Warburg element (W_3), indicating that the diffusion process is involved in the corrosion mechanism [17]. In this study, the polarization resistances (R_p) of the test materials were calculated as $R_p = R_1 + R_2$, where R_1 and R_2 represent the oxide film resistance and charge transfer resistance, respectively [27, 28]. The calculated R_p values are given in Table 3. It can be observed that the polarization resistance of Cu is one order lower than that of other materials.

4. Conclusions

Electrochemical characterization of various canister materials was performed using KURT groundwater with the addition of chloride ions. The corrosion potential and corrosion current of the test materials (SS316L, Ti-Gr.2, Alloy 22, and Cu) were measured using the polarization technique. The presence of chloride ions lowered the corrosion potential of SS316L and Cu. From the impedance measurements, we determined that Cu has a higher initial corrosion susceptibility than SS316L, Ti-Gr.2, and Alloy 22; in particular, the polarization resistance of Cu in the groundwater solution containing chloride ions is one order lower than that of other materials.

Data Availability

The data used to support the findings of this study are included within the article.

Conflicts of Interest

The authors declare that there are no conflicts of interest regarding the publication of this paper.

Acknowledgments

This study was supported by the Institute for Korea Spent Nuclear Fuel (iKSNF) and the National Research Foundation of Korea (NRF) grant funded by the Korean Government (Ministry of Science and ICT, MSIT) (2021M2E1A1085193 and 2021M2E3A2041351).

References

- [1] D. G. Bennett and R. Gens, "Overview of European concepts for high-level waste and spent fuel disposal with special reference waste container corrosion," *Journal of Nuclear Materials*, vol. 379, pp. 1–8, 2008.
- [2] R. Gubner and U. Andersson, *Corrosion Resistance of Copper Canister Weld Material*, 2007.
- [3] T. Hedman, A. Nystrom, and C. Thegerstrom, "Swedish containers for disposal of spent nuclear fuel and radioactive waste," *Comptes Rendus Physique*, vol. 3, pp. 903–913, 2002.
- [4] F. King, L. Ahonen, and C. Taxen, *Copper Corrosion under Expected Conditions in a Deep Geological Repository*, SKB TR-01-23, Stockholm, Sweden, 2001.
- [5] F. King, C. Lilja, and M. Vahanen, "Progress in the understanding of the long-term corrosion behaviour of copper canisters," *Journal of Nuclear Materials*, vol. 438, pp. 228–237, 2013.
- [6] S. Singh, M. Kumar, G. P. S. Sodhi, R. K. Buddu, and H. Singh, "Development of thick copper claddings on SS316L steel for In-vessel components of fusion reactors and copper-cast iron canisters," *Fusion Engineering and Design*, vol. 128, pp. 126–137, 2018.
- [7] N. Diomidis and F. King, *The Corrosion of Radioactive Waste Disposal Canisters Based on in Situ Test*, *Nuclear Corrosion, Research, Progress and Challenges*, 2020.
- [8] I. Soroka, N. Chae, and M. Jonsson, "On the mechanism of γ -radiation-induced corrosion of copper in water," *Corrosion Science*, vol. 182, pp. 109279–109283, 2021.
- [9] M. Bojinov, T. Ikalainen, and T. Saario, "Re-passivation rate and conduction mechanism of surface film on copper in nitrite solutions," *Corrosion Science*, vol. 205, pp. 110447–110455, 2022.
- [10] G. Kim, J. Jang, M. Lee, and S. Yeon, *Electrochemical Corrosion Characterization of Commercial Material (SS316L, Ni Alloy 22, and Ti Grade 2) in KURT Groundwater Solution*, 2021.
- [11] A. Hugot-Le-Goff, "Structure of very thin TiO_2 films studied by Ramam spectroscopy with interference enhancement," *Thin Solid Films*, vol. 142, no. 2, pp. 193–197, 1986.
- [12] T. Li, G. Huang, Y. Feng et al., "Effects of different ions and temperature on corrosion behavior of pure iron in anoxic simulated groundwater," *Materials*, vol. 13, no. 12, pp. 2713–2730, 2020.
- [13] R. Rosliza, W. B. Wan Nik, and H. B. Senin, "The effect of inhibitor on the corrosion of aluminum alloys in acidic solutions," *Materials Chemistry and Physics*, vol. 107, pp. 281–288, 2008.
- [14] H. Luo, H. Su, B. Li, and G. Ying, "Electrochemical and passive behaviour of tin alloyed ferritic stainless steel in concrete environment," *Applied Surface Science*, vol. 439, pp. 232–239, 2018.
- [15] Q. Zhang, M. Zheng, Y. Huang et al., "Long term corrosion estimation of carbon steel, titanium and its alloy in backfill material of compacted bentonite for nuclear waste repository," *Scientific Reports*, vol. 9, no. 1, pp. 3195–3212, 2019.
- [16] Y. V. Ingelgem, A. Hubin, and J. Vereecken, "Investigation of the first stages of the localized corrosion of pure copper combining EIS, FE-SEM and FE-AES," *Electrochimica Acta*, vol. 52, pp. 7642–7650, 2007.
- [17] W. A. Badawy, K. M. Ismail, and A. M. Fathi, "Effect of Ni content on the corrosion behavior of Cu-Ni alloys in neutral chloride solutions," *Electrochimica Acta*, vol. 50, no. 18, pp. 3603–3608, 2005.

- [18] I. D. Raistrick, J. R. MacDonald, and D. R. Franschetti, *Impedance Spectroscopy Emphasizing Solid Materials and Systems*, John Wiley & Sons, Hoboken, NJ, USA, 1987.
- [19] A. M. Fenelon and C. B. Breslin, "The electrochemical synthesis of polypyrrole at a copper electrode: corrosion protection properties," *Electrochimica Acta*, vol. 47, no. 28, pp. 4467–4476, 2002.
- [20] E. M. Sherif and S. M. Park, "Inhibition of copper corrosion in 3.0% NaCl solution by N Phenyl-1,4 phenyldiamine," *Journal of the Electrochemical Society*, vol. 152, no. 10, pp. B428–B433, 2005.
- [21] K. Rahmouni, M. Keddam, A. Srhiri, and H. Takenouti, "Corrosion of copper in 3% NaCl solution polluted by sulphide ions," *Corrosion Science*, vol. 47, no. 12, pp. 3249–3266, 2005.
- [22] G. Cicileo, B. Rosales, F. Varela, and J. Vilche, "Comparative study of organic inhibitors of copper corrosion," *Corrosion Science*, vol. 41, no. 7, pp. 1359–1375, 1999.
- [23] A. Palit and S. O. Pehkonen, "Copper corrosion in distribution systems: evaluation of a homogeneous Cu₂O film and a natural corrosion scale as corrosion inhibitors," *Corrosion Science*, vol. 42, no. 10, pp. 1801–1822, 2000.
- [24] B. Trachli, M. Keddam, H. Takenouti, and A. Srhiri, "Protective effect of electropolymerized 3-amino 1,2,4-triazole towards corrosion of copper in 0.5 M NaCl," *Corrosion Science*, vol. 44, no. 5, pp. 997–1008, 2002.
- [25] C. Deslouis, B. Tribollet, G. Mengoli, and M. M. Musiani, "Electrochemical behaviour of copper in neutral aerated chloride solution II Impedance investigation," *Journal of Applied Electrochemistry*, vol. 18, no. 3, pp. 384–393, 1988.
- [26] T. Tuken, B. Yazici, and M. Erbil, "Polypyrrole/polythiophene coating for copper protection," *Progress in Organic Coatings*, vol. 53, no. 1, pp. 38–45, 2005.
- [27] M. Galai, H. Benqlilou, M. E. Touhami, T. Belhaj, K. Berrami, and H. E. Kafssaoui, "Comparative analysis for the corrosion susceptibility of copper alloys in sandy soil," *Environmental Engineering Research*, vol. 23, no. 2, pp. 164–174, 2018.
- [28] A. Bacelis, L. Veleva, and M. A. Alpuche-Aviles, "Copper corrosion behavior in simulated concrete-pore solutions," *Metals*, vol. 10, no. 4, pp. 474–493, 2020.